JOURNAL OF THERMOPHYSICS AND HEAT TRANSFER
Vol. 18, No. 4, October–December 2004

Natural Convection in Rectangular Layered Porous Cavities

J. C. Leong* and F. C. Lai†
University of Oklahoma, Norman, Oklahoma 73019

A numerical study was performed to further investigate the flow and temperature fields in layered porous cavity. The cavities considered have an aspect ratio of either 0.2 (shallow cavities) or 5 (tall cavities) with two or four sublayers. Similar to the case of square cavities, convection is always initiated in the more permeable sublayer. As the base Rayleigh number increases, the strength of the convective cell increases and leads to flow penetration to the less permeable sublayer. The results obtained were used to evaluate the validity of the boundary-layer assumption employed by other investigators. In addition, they were used to examine the feasibility of extending the lumped-system analysis from square cavities to rectangular ones. The averaging schemes in defining the effective permeability, as suggested in the previous study for a square cavity, were tested.

Nomenclature

A	=	aspect ratio, H/L
c_p	=	heat capacity, J/kg · K
g	=	gravitational acceleration, m/s^2
H	=	height of cavity, m
H_1	=	location of the interface of horizontal sublayers, m
K	=	permeability, m^2
K_A	=	effective permeability of horizontal layers, m^2
K_H	=	effective permeability of vertical layers, m^2
$\tilde{K}$	=	permeability ratio, K_2/K_1
k	=	effective thermal conductivity of porous medium, W/m · K
L	=	width of cavity, m
L_1	=	location of the interface of vertical sublayers, m
N	=	nodal number of the layer interface
Nu	=	average Nusselt number, hL/k
p	=	pressure, Pa
Ra_1	=	base Rayleigh number, $K_1 g\beta(T_h - T_c)L/\alpha\nu$
T	=	temperature, K
u, v	=	Darcy velocity in the x and y directions, m/s
X, Y	=	dimensionless Cartesian coordinates, x/L, y/H
x, y	=	Cartesian coordinates, m
α	=	effective thermal diffusivity of porous medium, $k/(\rho c_p)_f$, m^2/s
β	=	thermal expansion coefficient, $(-1/\rho)(\partial\rho/\partial T)_p$, K^{-1}
θ	=	dimensionless temperature, $(T - T_c)/(T_h - T_c)$
μ	=	dynamic viscosity of fluid, kg/m · s
ν	=	kinematic viscosity of fluid, m^2/s
ρ	=	fluid density, kg/m^3
Ψ	=	dimensionless stream function

Subscripts

c	=	cold wall
f	=	fluid
h	=	hot wall
i	=	index of sublayer (1, 2, . . .)

Received 6 June 2003; revision received 28 June 2004; accepted for publication 1 July 2004.

*Graduate Research Assistant, School of Aerospace and Mechanical Engineering; currently Assistant Professor, Department of Vehicle Engineering, National Pingtung University of Science and Technology, Taiwan. Student Member AIAA.

†Associate Professor, School of Aerospace and Mechanical Engineering. Senior Member AIAA.

Introduction

HEAT transfer in porous media has many important applications in engineering. As a result, extensive research has been conducted in the past three decades. However, most previous studies have focused on homogenous porous media, whereas layered porous media, although encountered more frequently in applications, have received rather little attention. For stability analysis, Masuoka et al.[1] made the first study on the onset of thermal convection in a two-layer porous system. Their work was later extended by McKibbin and O'Sullivan[2] to multilayer systems. Rees and Riley[3] further extended the classical stability problem into a three-dimensional domain. For heat-transfer analysis, Donaldson[4] reported the first numerical result of heat convection in a multilayer system. This was followed by Rana et al.[5] in numerical simulation of a geothermal reservoir using a layered porous model. Their results compared favorably with the field data obtained. For horizontal layers, heat-transfer results have been presented by McKibbin[6] as well as McKibbin and Tyvand.[7,8] For vertical layers, Poulikakos and Bejan[9] as well as Lai and Kulacki[10] have studied the effects of permeability contrast and thermal conductivity ratio on natural convection in two- or three-layer porous systems. For layered porous annuli, Muralidhar et al.[11] have presented both experimental and numerical results. Pan and Lai[12] later refined the work of Muralidhar et al.[11] and were able to explain the discrepancy found between the numerical and experimental results reported by Muralidhar et al.[11]

Based on the boundary-layer approximation, Rees[13] has recently performed an analytical study on natural convection from a heated surface in a semi-infinite porous medium. Although some interesting results were brought out from this study, it is noticed that the results have serious limitations in application because of the assumption made. To have a valid boundary-layer assumption in the previous analysis, the Rayleigh number involved has to be very large ($Ra \gg 1$), and the permeability ratio is greater than unity. For applications involving an intermediate Rayleigh number, the boundary-layer assumption might not be satisfied. Also, the permeability ratio between two neighboring sublayers can be greater or less than unity. Because of these constraints, the previous results have rather limited applications. With the relaxation of the boundary-layer assumptions made in the previous study,[13] the present numerical results can be more useful for engineers. In addition, the present study examines the feasibility of extending the lumped-system analysis for heat transfer in layered porous media, as proposed by Leong and Lai,[14] from square cavities to rectangular ones. The proposed lumped-system analysis uses an effective permeability to represent a layered porous medium and treats the medium as if it were homogeneous. Clearly, if the proposed approach proves applicable, it can significantly reduce the computational effort when dealing with heat transfer in layered porous media. The averaging schemes that they proposed in defining the effective permeability are tested in the present study. To validate the lumped-system model, the present

results are also compared with those obtained from homogeneous systems.

Formulation

The cavity considered is either tall ($A = 5$) or shallow ($A = 0.2$), as shown in Fig. 1. The aspect ratios chosen for the cavity best present the geometry considered. The cavity consists of two or four sublayers of equal thickness but with distinct permeabilities. For the four-layer case, the permeabilities of these sublayers are alternating among the sublayers (i.e., $K_1 = K_3$ and $K_2 = K_4$). Layered porous cavities with alternating permeability represent the most fundamental system in nonhomogeneous porous media, and the results obtained from this system can later be generalized to more complicated systems as demonstrated by McKibbin and Tyvand.[7,8] The sublayers are assumed saturated with the same fluid. The cavity walls are impermeable. The top and bottom walls are insulated while the vertical walls are differentially heated at constant temperatures T_h and T_c ($T_h > T_c$). The governing equations based on Darcy's law are given by Leong and Lai[14]:

$$\frac{\partial u_i}{\partial x} + \frac{\partial v_i}{\partial y} = 0 \tag{1}$$

$$u_i = -\frac{K_i}{\mu}\frac{\partial p_i}{\partial x} \tag{2}$$

$$v_i = -\frac{K_i}{\mu}\left(\frac{\partial p_i}{\partial y} + \rho_i g\right) \tag{3}$$

$$u_i\frac{\partial T_i}{\partial x} + v_i\frac{\partial T_i}{\partial y} = \alpha_i\left(\frac{\partial^2 T_i}{\partial x^2} + \frac{\partial^2 T_i}{\partial y^2}\right) \tag{4}$$

In addition to the boundary conditions, interface conditions are required for the solution of the flow and temperature fields in the cavity. The interface conditions imposed are the continuity of mass, pressure, temperature, and heat flux across the interface. McKibbin and O'Sullivan[2] as well as Rana et al.[5] have justified the use of these conditions. For brevity, the boundary and interface conditions are presented here only for a two-layer cavity, but can be extended to a four-layer case in a similar fashion.

1) Vertical sublayers:

$$x = 0, \qquad u_1 = 0, \qquad T_1 = T_h \tag{5a}$$

$$x = L, \qquad u_2 = 0, \qquad T_2 = T_c \tag{5b}$$

$$x = L_1, \qquad u_1 = u_2, \qquad p_1 = p_2$$
$$T_1 = T_2, \qquad k_1\frac{\partial T_1}{\partial x} = k_2\frac{\partial T_2}{\partial x} \tag{5c}$$

$$y = 0, \quad x < L_1, \quad v_1 = 0, \quad \frac{\partial T_1}{\partial y} = 0$$
$$x > L_1, \quad v_2 = 0, \quad \frac{\partial T_2}{\partial y} = 0 \tag{5d}$$

$$y = H, \quad x < L_1, \quad v_1 = 0, \quad \frac{\partial T_1}{\partial y} = 0$$
$$x > L_1, \quad v_2 = 0, \quad \frac{\partial T_2}{\partial y} = 0 \tag{5e}$$

2) Horizontal sublayers:

$$x = 0, \quad y < H_1, \quad u_1 = 0, \quad T_1 = T_h$$
$$y > H_1, \quad u_2 = 0, \quad T_2 = T_h \tag{6a}$$

$$x = L, \quad y < H_1, \quad u_1 = 0, \quad T_1 = T_c$$
$$y > H_1, \quad u_2 = 0, \quad T_2 = T_c \tag{6b}$$

$$y = 0, \quad v_1 = 0, \quad \frac{\partial T_1}{\partial y} = 0 \tag{6c}$$

$$y = H, \quad v_2 = 0, \quad \frac{\partial T_2}{\partial y} = 0 \tag{6d}$$

$$y = H_1, \quad v_1 = v_2, \quad p_1 = p_2$$
$$T_1 = T_2, \quad k_1\frac{\partial T_1}{\partial y} = k_2\frac{\partial T_2}{\partial y} \tag{6e}$$

Equations (1–6) can be simplified by introducing the stream function. In dimensionless form, they are given by

$$\frac{\partial^2 \Psi_i}{\partial X^2} + \frac{1}{A^2}\frac{\partial^2 \Psi_i}{\partial Y^2} = -Ra_i\frac{\partial \theta_i}{\partial X} \tag{7}$$

$$\frac{\partial \Psi_i}{\partial Y}\frac{\partial \theta_i}{\partial X} - \frac{\partial \Psi_i}{\partial X}\frac{\partial \theta_i}{\partial Y} = A\frac{\partial^2 \theta_i}{\partial X^2} + \frac{1}{A}\frac{\partial^2 \theta_i}{\partial Y^2} \tag{8}$$

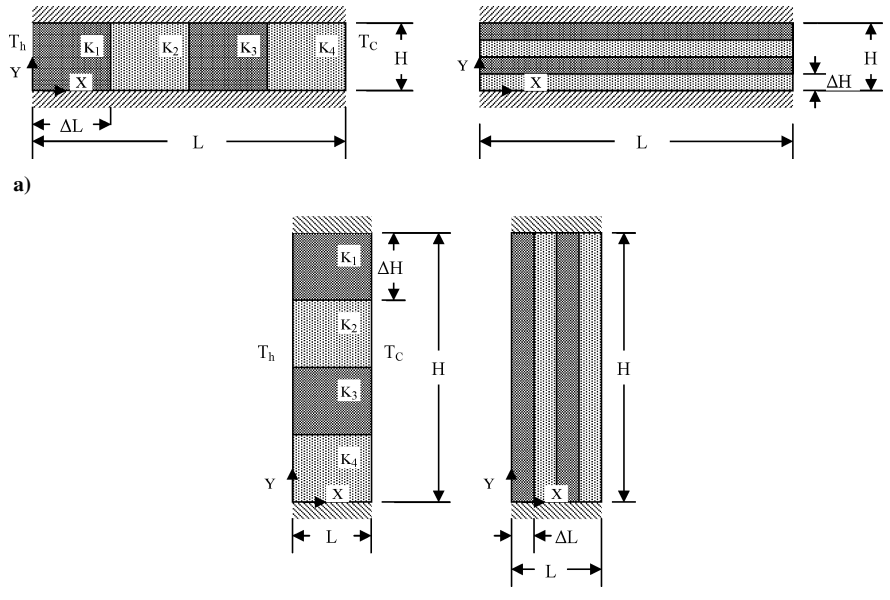

Fig. 1 Layered porous cavities with four sublayers subject to differential heating from vertical walls: a) shallow cavities ($A = 0.2$) and b) tall cavities ($A = 5$).

where

$$\alpha_i = \frac{k_i}{(\rho c_p)_f}, \qquad Ra_i = \frac{K_i g\beta(T_h - T_c)L}{\alpha_i \nu_i} \tag{9}$$

Because the porous layers are saturated with the same fluid (thus, $\nu_1 = \nu_2$ and $\alpha_1 = \alpha_2$), the ratio of Rayleigh numbers can be obtained as

$$\frac{Ra_1}{Ra_2} = \frac{K_1}{K_2} \tag{10}$$

For the convenience of discussion and reference, Ra_1, which is based on the properties of the first sublayer, is named the base Rayleigh number.

The corresponding boundary and interface conditions are expressed next:

1) Vertical sublayers:

$$X = 0, \qquad \Psi_1 = 0, \qquad \theta_1 = 1 \tag{11a}$$

$$X = 1, \qquad \Psi_2 = 0, \qquad \theta_2 = 0 \tag{11b}$$

$$X = \frac{L_1}{L}, \qquad \Psi_1 = \frac{\alpha_2}{\alpha_1}\Psi_2, \qquad \frac{\partial \Psi_1}{\partial X} = \frac{K_1}{K_2}\frac{\alpha_2}{\alpha_1}\frac{\partial \Psi_2}{\partial X}$$

$$\theta_1 = \theta_2, \qquad \frac{\partial \theta_1}{\partial X} = \frac{k_2}{k_1}\frac{\partial \theta_2}{\partial X} \tag{11c}$$

$$Y = 0, \qquad X < \frac{L_1}{L}, \qquad \Psi_1 = 0, \qquad \frac{\partial \theta_1}{\partial Y} = 0$$

$$X > \frac{L_1}{L}, \qquad \Psi_2 = 0, \qquad \frac{\partial \theta_2}{\partial Y} = 0 \tag{11d}$$

$$Y = 1, \qquad X < \frac{L_1}{L}, \qquad \Psi_1 = 0, \qquad \frac{\partial \theta_1}{\partial Y} = 0$$

$$X > \frac{L_1}{L}, \qquad \Psi_2 = 0, \qquad \frac{\partial \theta_2}{\partial Y} = 0 \tag{11e}$$

2) Horizontal sublayers:

$$X = 0, \qquad Y < \frac{H_1}{H}, \qquad \Psi_1 = 0, \qquad \theta_1 = 1$$

$$Y > \frac{H_1}{H}, \qquad \Psi_2 = 0, \qquad \theta_2 = 1 \tag{12a}$$

$$X = 1, \qquad Y < \frac{H_1}{H}, \qquad \Psi_1 = 0, \qquad \theta_1 = 0$$

$$Y > \frac{H_1}{H}, \qquad \Psi_2 = 0, \qquad \theta_2 = 0 \tag{12b}$$

$$Y = 0, \qquad \Psi_1 = 0, \qquad \frac{\partial \theta_1}{\partial Y} = 0 \tag{12c}$$

$$Y = 1, \qquad \Psi_2 = 0, \qquad \frac{\partial \theta_2}{\partial Y} = 0 \tag{12d}$$

$$Y = \frac{H_1}{H}, \qquad \Psi_1 = \frac{\alpha_2}{\alpha_1}\Psi_2, \qquad \frac{\partial \Psi_1}{\partial Y} = \frac{K_1}{K_2}\frac{\alpha_2}{\alpha_1}\frac{\partial \Psi_2}{\partial Y}$$

$$\theta_1 = \theta_2, \qquad \frac{\partial \theta_1}{\partial Y} = \frac{k_2}{k_1}\frac{\partial \theta_2}{\partial Y} \tag{12e}$$

The interface conditions have been implemented using imaginary nodal points as described by Rana et al.[5] The equations for the interface stream function and dimensionless temperature are given next:

1) Vertical sublayers:

$$\Psi^1_{N,j} = \frac{A^2}{A^2+1}\frac{\tilde{K}}{\tilde{K}+1}\Psi^1_{N-1,j} + \frac{A^2}{A^2+1}\frac{1}{\tilde{K}+1}\Psi^2_{N+1,j} + \frac{1}{2(A^2+1)}\left(\Psi^1_{N,j-1} + \Psi^1_{N,j+1}\right) + \frac{A^2}{4(A^2+1)}\frac{\tilde{K}}{\tilde{K}+1} \times Ra_1\left(\theta^1_{N-2,j} - 4\theta^1_{N-1,j} + 4\theta^2_{N+1,j} - \theta^2_{N+2,j}\right)\Delta X \tag{13a}$$

$$\theta^1_{N,j} = \theta^2_{N,j} = \frac{1}{3}\frac{4\left(\theta^1_{N-1,j} + \theta^2_{N+1,j}\right) - \left(\theta^1_{N-2,j} + \theta^2_{N+2,j}\right)}{2} \tag{13b}$$

2) Horizontal sublayers:

$$\Psi^1_{i,N} = \frac{1}{A^2+1}\frac{\tilde{K}}{\tilde{K}+1}\Psi^1_{i,N+1} + \frac{1}{A^2+1}\frac{1}{\tilde{K}+1}\Psi^2_{i,N-1} + \frac{A^2}{2(A^2+1)}\left(\Psi^1_{i-1,N} + \Psi^1_{i+1,N}\right) + \frac{A^2}{2(A^2+1)}\frac{\tilde{K}}{\tilde{K}+1}Ra_1\left(\theta^1_{i+1,N} - \theta^1_{i-1,N}\right)\Delta X \tag{14a}$$

$$\theta^1_{i,N} = \theta^2_{i,N} = \frac{1}{3}\frac{4\left(\theta^1_{i,N+1} + \theta^2_{i,N-1}\right) - \left(\theta^1_{i,N+2} + \theta^2_{i,N-2}\right)}{2} \tag{14b}$$

where $\tilde{K} = K_2/K_1$ is the permeability ratio.

The governing equations with the boundary and interface conditions were solved using a finite difference method. This method has been successfully employed by the authors for similar studies.[10,14] Uniform grids (201×41 for $A = 0.2$ and 41×201 for $A = 5$) with under- and overrelaxation are used for most of the calculations to ensure the efficiency and accuracy of the numerical results. For the case of $K_1/K_2 = 0.01$, finer grids (301×61 for $A = 0.2$, and 301×1501 for $A = 5$) are normally required. Note that further refinement of the grid does not significantly improve the results. For example, the change in the average Nusselt number is less than 0.5% when the grids change from 201×41 to 401×81 for shallow cavities ($A = 0.2$) and 41×201 to 81×401 for tall cavities ($A = 5$) at $Ra_1 = 100$. An overall energy balance has been performed in each calculation to further evaluate the accuracy of the results obtained. For the present study, the results are satisfied within 3% (most are within 1%). The overall heat transfer is expressed in terms of the average Nusselt number at each vertical wall as given by

$$\overline{Nu} = -\frac{1}{A}\int_0^1 \left.\frac{\partial \theta}{\partial X}\right|_{X=0,1} dY \tag{15}$$

Results and Discussions

For natural convection in a homogeneous porous cavity, the flow development with increase in the Rayleigh number has been classified by Prasad and Kulacki[15] into four regimes: conduction, asymptotic flow, pseudo boundary-layer flow, and boundary-layer flow. Although the conduction regime is characterized by a moderate circulatory parallel flow structure and a temperature profile linearly distributed in the x direction, the asymptotic flow regime is identified by a gradual temperature stratification in the core region and an increase in heat transfer by convection near the walls. Further increase in the Rayleigh number leads to the boundary-layer flow regime. The distinction between the pseudo boundary-layer and boundary-layer flow regimes is the contribution of heat transfer by conduction in the core region. For the former case, conduction in the core region is not negligible at high Rayleigh numbers even though the heat transfer is mainly by convection through boundary layers along the walls. Also, in the boundary-layer flow regime heat-transfer results in terms of the Nusselt number become almost independent of the aspect ratio. These classifications are very useful for the discussion that follows.

Layered Tall Cavities

From the results obtained, it is observed that convection always starts in the more permeable sublayer(s) and penetrates the less permeable sublayer(s) as the base Rayleigh number increases (Figs. 2 and 3). The Rayleigh numbers in the figures are chosen to best

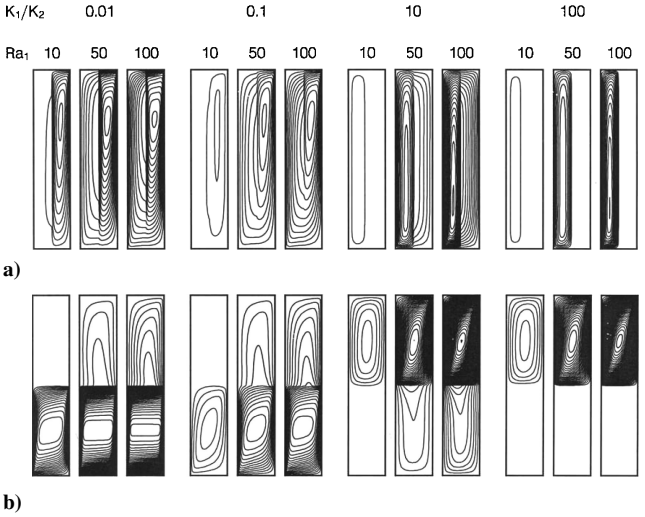

Fig. 2 Flowfields in a tall porous cavity with two sublayers ($\Delta\Psi = 2$ for $K_1/K_2 < 1$ and $\Delta\Psi = 0.2$ for $K_1/K_2 > 1$).

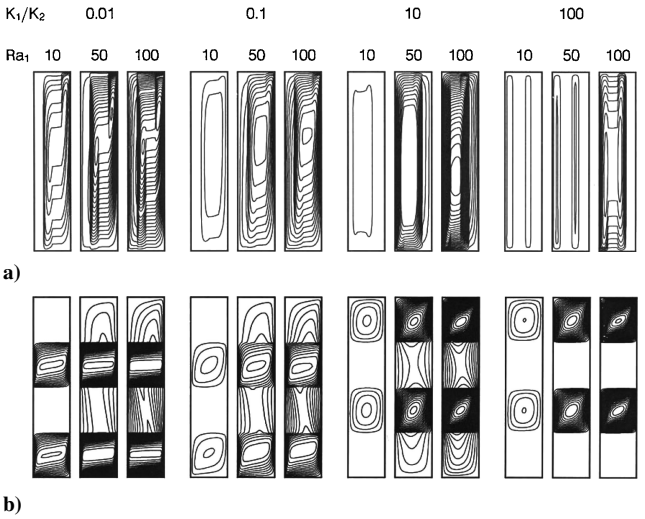

Fig. 3 Flowfields in a tall porous cavity with four sublayers: a) vertical sublayers and b) horizontal sublayers ($\Delta\Psi = 2$ for $K_1/K_2 < 1$ and $\Delta\Psi = 0.2$ for $K_1/K_2 > 1$, except $\Delta\Psi = 0.05$ for $K_1/K_2 > 1$ and $Ra_1 = 10$ in Fig. 3a).

present the transition of heat-transfer regimes and flow structures. The dotted lines in the figures show the location of sublayer interface. For tall cavities with vertical sublayers (Fig. 2), the presence of boundary layers can be clearly observed through the close packing of streamlines. Boundary layers develop not only along the vertical walls but also along the layer interfaces. This is most obvious when the sublayers have a large permeability contrast and are at a high Rayleigh number.

Also noticed is that, for a given base Rayleigh number, the strength of convective cell decreases with the sublayer permeability ratio. For cavities with two sublayers, there is only one convective cell. However, two secondary cells appear in cavities with four sublayers when the permeability contrast is large (e.g., for $K_1/K_2 = 0.01$ and 100 at $Ra_1 = 100$). Clearly, these two secondary cells are split from the primary cell as a result of the presence of the less permeable sublayer in between. For cavities with four sublayers (Fig. 3), it is interesting to observe that the flow direction in the sandwiched less permeable sublayer is nearly horizontal while it is mainly vertical in other sublayers (e.g., for $K_1/K_2 = 0.01$). When generalized to a multilayer porous medium, this implies that the satisfaction of boundary-layer approximation in one sublayer (locally) does not always guarantee the satisfaction of that approximation in all sublayers (globally). This can also be observed from the result presented by Rees[13] in which the streamline pattern in a multiply layered medium clearly shows a contradiction to the boundary-layer assumption (in which the horizontal velocity component is not negligibly small when compared to the vertical velocity component).

For tall cavities with horizontal sublayers (Figs. 2b and 3b), the flow pattern in the more permeable sublayer(s) resembles that in a homogeneous cavity with an aspect ratio of 2.5 (for two sublayers) and 1.25 (for four sublayers). Recall that $Ra_2 (= Ra_4) = Ra_1 (K_2/K_1)$. For $K_1/K_2 < 1$, the corresponding Rayleigh number for the more permeable sublayer(s) is actually higher than the base Rayleigh number such that the flow in these sublayer(s) is mainly in the boundary-layer regime (according to the classification of Prasad and Kulacki[15]). In contrast, the flow in the more permeable sublayer(s) of cavities with $K_1/K_2 > 1$ is in the asymptotic flow regime at most. For cavities with four sublayers, the flow patterns in the more permeable sublayers, although similar, are not exactly identical. This is attributed to the difference in the thermal boundary conditions. For $K_1/K_2 < 1$, the lower cell is subject to an insulated boundary while the upper cell is not. The situation is just reversed for $K_1/K_2 > 1$. Because of the nature of buoyancy, flow penetration is minimum for sublayers with $K_1/K_2 = 0.01$. The strength of convective cells in tall cavities with horizontal sublayers (Figs. 2b and 3b) is found to be greater than those with vertical sublayers (Figs. 2a and 3a). This has led to a conclusion that maximum convection occurs in a sublayer for which its aspect ratio is close to unity. A similar conclusion has been drawn by Prasad and Kulacki[15] for natural convection in homogeneous porous cavities.

For cavities with horizontal sublayers, energy transfer from the hot wall to the cold wall takes place simultaneously through each sublayer (i.e., in a parallel fashion) with most of the contribution being by convection through the more permeable sublayer(s). This is different from cavities with vertical sublayers where energy must transfer through each sublayer in sequence. For this reason, the strength of convective cells in the cavities with horizontal sublayers is greater than that in the cavities with vertical sublayers. Consequently, it is expected that heat transfer from cavities with horizontal sublayers is higher than those with vertical sublayers.

Because conduction is characterized by uniform distributed isotherms, the heat-transfer mode in each sublayer can be easily identified from the isotherm pattern in a given cavity (Figs. 4 and 5). For $K_1/K_2 < 1$, convection always prevails in the more permeable sublayer(s), whereas conduction is the initial mode of heat transfer in the less permeable sublayer and gradually evolves to convection as the base Rayleigh number increases. Also, thermal stratification is commonly found in the more permeable sublayer for $K_1/K_2 < 1$ (e.g., $K_1/K_2 = 0.01$ in Figs. 4b and 5b). However, thermal

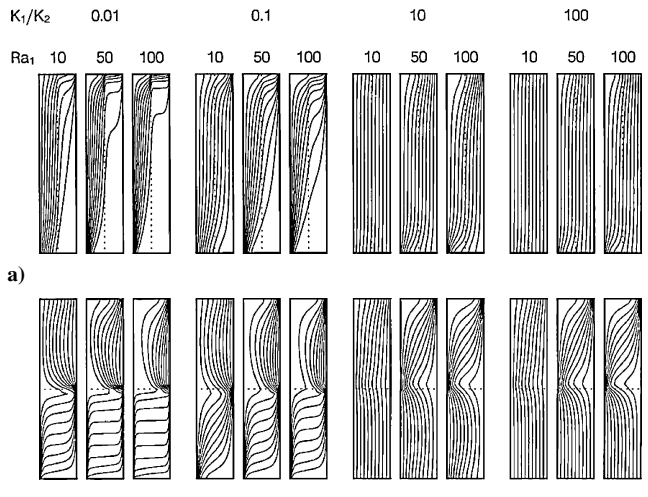

Fig. 4 Temperature fields in a tall porous cavity with two sublayers: a) vertical sublayers and b) horizontal sublayers ($\Delta\theta > 0.1$).

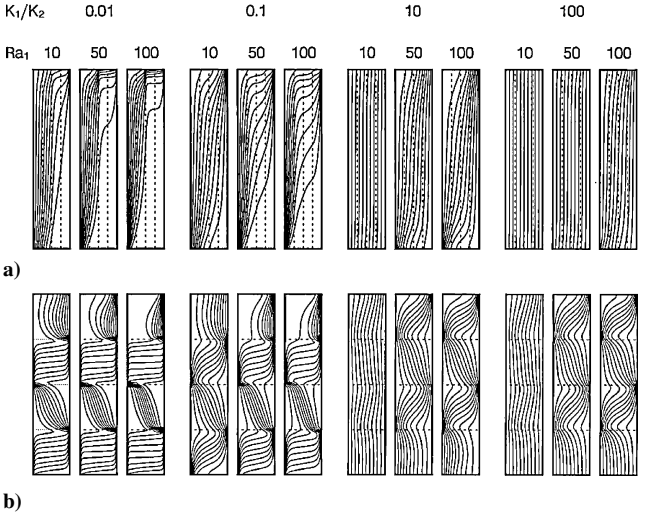

Fig. 5 Temperature fields in a tall porous cavity with four sublayers: a) vertical sublayers and b) horizontal sublayers ($\Delta\theta = 0.1$).

stratification is better maintained in the cavities with horizontal sublayers than those with vertical sublayers. From the isotherm patterns, it is easy to identify that the convective flow in cavities of $K_1/K_2 < 1$ is mostly in the boundary-layer flow regime (which is characterized by a nonuniform, nonlinear isotherm pattern and a large temperature gradient at wall) while it is in the conduction and asymptotic flow regimes for cavities of $K_1/K_2 > 1$. For tall cavities with vertical sublayers and a small permeability ratio (Fig. 4), the thermal boundary layer can be clearly observed to develop along the walls. However, this characteristic does not extend too far into other sublayers, which makes the boundary-layer assumption not uniformly valid. Also noticed is that thermal stratification is better developed in sublayers with a smaller permeability ratio. For a large permeability ratio, the almost evenly distributed isotherms indicate that heat transfer is mainly by conduction. Convection is further suppressed by an increase in the number of sublayers. For tall cavities with horizontal sublayers (Fig. 5b), isotherms indicate that convection is the primary heat-transfer mode for $K_1/K_2 < 1$. For cavities with two sublayers and a large permeability ratio, heat transfer is dominated by convection through the more permeable sublayer and conduction through the less permeable sublayer. With an increase in the number of sublayers, heat transfer is increased by weak convection in the sandwiched less permeable sublayer as evident from the isotherm patterns (Fig. 5b).

Layered Shallow Cavities

For shallow cavities with vertical sublayers, convection also starts from the more permeable sublayer(s) and penetrates the less permeable sublayer(s) when the base Rayleigh number increases (Figs. 6 and 7). It is recognized that the flow pattern in the more permeable sublayer(s) bears some similarities to that in a homogeneous cavity with an aspect ratio of 0.4 (for two sublayers) and 0.8 (for 4 sublayers).[15] Also noticed is that convection is slightly suppressed by an increase in the number of sublayers. For $K_1/K_2 < 1$, the flow development can be clearly observed from conduction, asymptotic flow, and pseudo boundary-layer to boundary-layer flow regimes as the base Rayleigh number increases (Figs. 6a and 7a). Because convection is very weak in cavities of $K_1/K_2 > 1$, heat transfer remains mostly in the conduction regime. As a result, the strength and pattern of the convective cells are about the same, but flow penetration is only visible for $K_1/K_2 = 10$.

For shallow cavities with horizontal sublayers (Figs. 6b and 7b), the development of boundary-layer flow is mainly along the horizontal wall and the layer interface. In the case of two sublayers, the flow patterns in the more permeable sublayer resemble those in a homogeneous cavity with an aspect ration of 0.1 (Ref. 15), particularly for those at $K_1/K_2 = 0.01$ and 100. For $K_1/K_2 > 1$, the convective

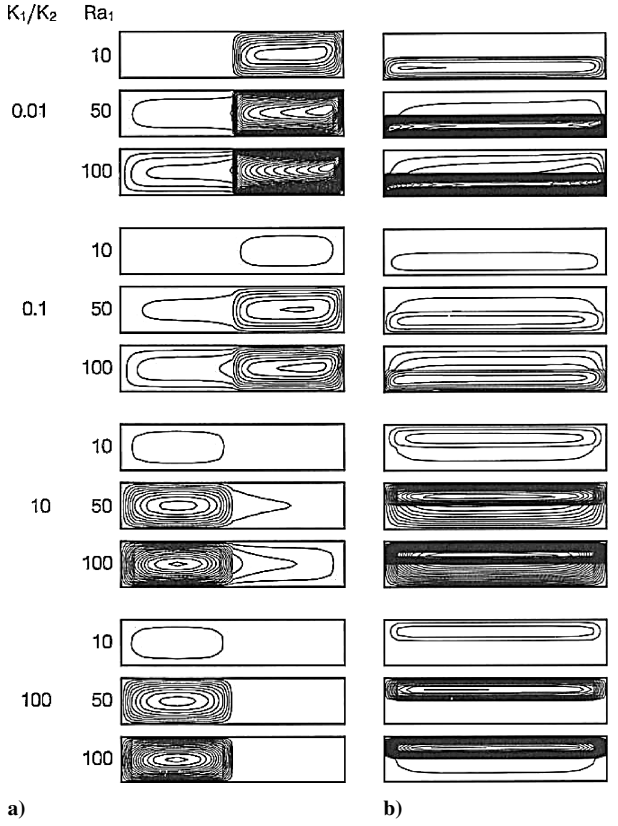

Fig. 6 Flowfields in a shallow porous cavity with two sublayers: a) vertical sublayers and b) horizontal sublayers ($\Delta\Psi = 0.25$ for $K_1/K_2 < 1$, except $\Delta\Psi = 0.1$ for $K_1/K_2 = 0.1$ and $Ra_1 = 10$ in Fig. 6b, $\Delta\Psi = 0.025$ for $K_1/K_2 = 10$, and $\Delta\Psi = 0.005$ for $K_1/K_2 = 100$).

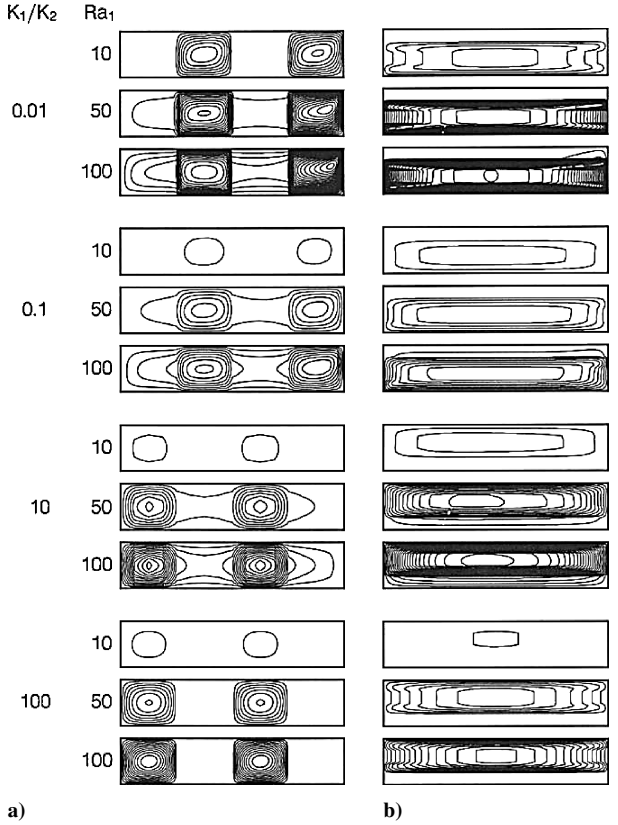

Fig. 7 Flowfields in a shallow porous cavity with four sublayers: a) vertical sublayers and b) horizontal sublayers ($\Delta\Psi = 0.25$ for $K_1/K_2 < 1$, except $\Delta\Psi = 0.1$ for $K_1/K_2 = 0.1$ and $Ra_1 = 10$ in Fig. 7b, $\Delta\Psi = 0.025$ for $K_1/K_2 = 10$, and $\Delta\Psi = 0.005$ for $K_1/K_2 = 100$).

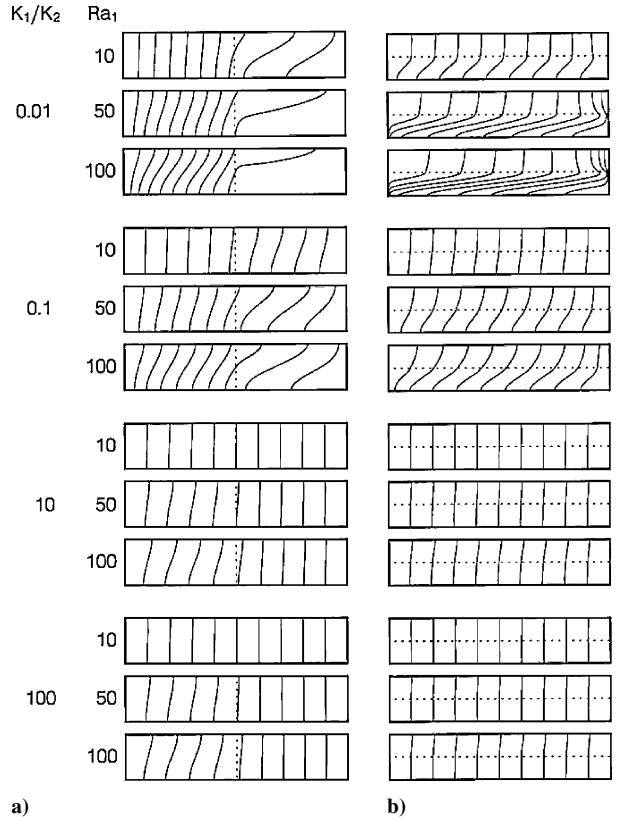

Fig. 8 Temperature fields in a shallow porous cavity with two sublayers: a) vertical sublayers and b) horizontal sublayers ($\Delta\theta = 0.1$).

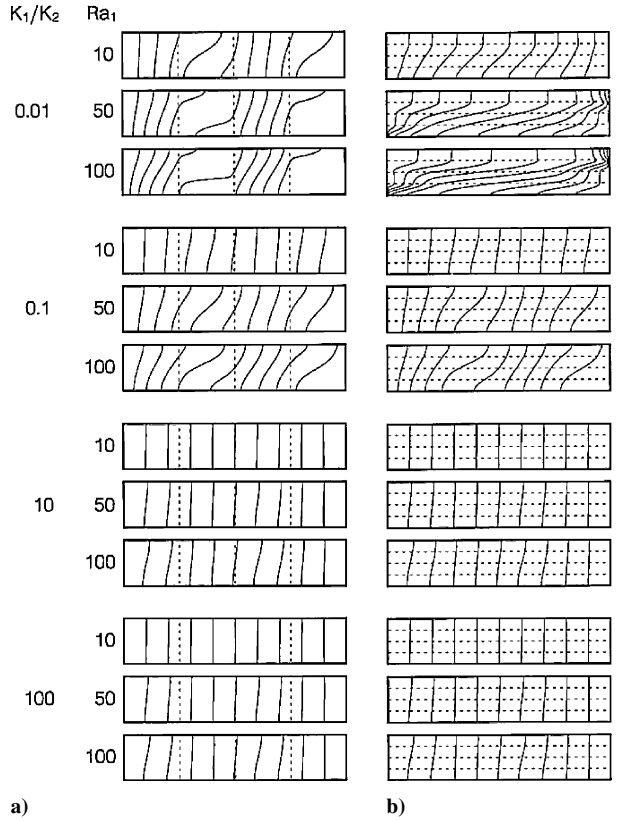

Fig. 9 Temperature fields in a shallow porous cavity with four sublayers: a) vertical sublayers and b) horizontal sublayers ($\Delta\theta = 0.1$).

flow is rather weak and is generally in the horizontal direction except in the vicinity of the vertical walls. Clearly, this falls into the category of the conduction regime. For $K_1/K_2 < 1$, convection is mainly confined in the lower (more permeable) sublayer (Fig. 6b). Two secondary cells appear in the lower sublayer for $K_1/K_2 = 0.01$ and $Ra \geq 50$. This is consistent with the results reported by Prasad and Kulacki.[15] They have shown that multicellular flow is only possible for a shallow cavity ($A < 1$), and its occurrence depends on the Rayleigh number and the aspect ratio of the cavity. For shallow cavities with four horizontal sublayers (Fig. 7b), the flow pattern is a stretch of that of two sublayers (Fig. 6b) with vertical flow in the sandwiched less permeable sublayer to bridge the convective cell in two more permeable sublayers.

From the isotherm patterns (Figs. 8 and 9), it is easy to recognize that conduction is the primary heat-transfer mode for cavities of $K_1/K_2 > 1$. Especially for $K_1/K_2 = 100$, the less permeable sublayer behaves like an impermeable partition that significantly suppresses convection. For $K_1/K_2 < 1$, convection is always dominant in the more permeable sublayer(s) (Fig. 8), and a transition of the heat-transfer mode from conduction to convection is observed in the less permeable sublayer as the Rayleigh number increases.

For shallow cavities with horizontal sublayers, convection is insignificant, and conduction again is the dominant heat-transfer mode for cavities of $K_1/K_2 > 1$. Because of conduction, the temperature profiles do not differ much from one case to the other (Fig. 9), that is, regardless of the permeability ratio and number of sublayers (as compared to Fig. 8). On the other hand, for cavities of $K_1/K_2 < 1$, from the isotherm patterns (particularly for $K_1/K_2 = 0.01$) a transition of flow in the more permeable sublayer from conduction to the pseudo boundary-layer regime can be clearly seen when the Rayleigh number increases (Figs. 8b and 9b). As the base Rayleigh number increases, the temperature field in the lower sublayer tends to stratify (Fig. 8b). Although heat transfer by convection increases through the boundary-layer flow, conduction through the core region is also important. As a result, only a horizontal thermal boundary layer is visible along the bottom wall.

Heat-Transfer Results

For heat-transfer results, it is found that the average Nusselt number for $K_1/K_2 < 1$ is always greater than that of a homogeneous layer, while it is always less than that of a homogeneous layer for $K_1/K_2 > 1$. This is consistent with the results reported by Lai and Kulacki[10] as well as Leong and Lai.[14] Also found is that the average Nusselt number for a shallow cavity of $K_1/K_2 > 1$ is almost constant, regardless of the sublayer orientation, number of sublayers, and their permeability ratio. The reason is that the heat transfer in these cases is predominantly by conduction.

To correlate the heat-transfer data for natural convection in layered porous cavities, it has been reported by Leong and Lai[14] that the use of effective permeability produces very nice results. According to their proposal, the heat-transfer results for natural convection in a layered porous cavity can be predicted with reasonably good accuracy using the correlation for a homogeneous cavity if the permeability of the homogeneous cavity is replaced by the effective permeability of the layered cavity. The effective permeability of a layered cavity depends on the layer structure. For a cavity with vertical sublayers, its effective permeability is given by[14]

$$1/K_H = \tfrac{1}{2}(1/K_1 + 1/K_2) \tag{16a}$$

For a cavity with horizontal sublayers, it is given by[14]

$$K_A = (K_1 + K_2)/2 \tag{16b}$$

Clearly, the preceding formulations are based on a concept similar to thermal resistance. Because the resistance to convective heat transfer is inversely proportional to the sublayer permeability, Eq. (16a) represents a thermal circuit in series, whereas Eq. (16b) represents a thermal circuit in parallel.

The heat-transfer results are shown in Figs. 10 (tall cavities) and 11 (shallow cavities) as a function of the effective Rayleigh number. For comparison, the results for a homogeneous cavity are also included (as solid lines) in the figures. It is found that the heat-transfer results for cavities with various layered structures fall nicely on the

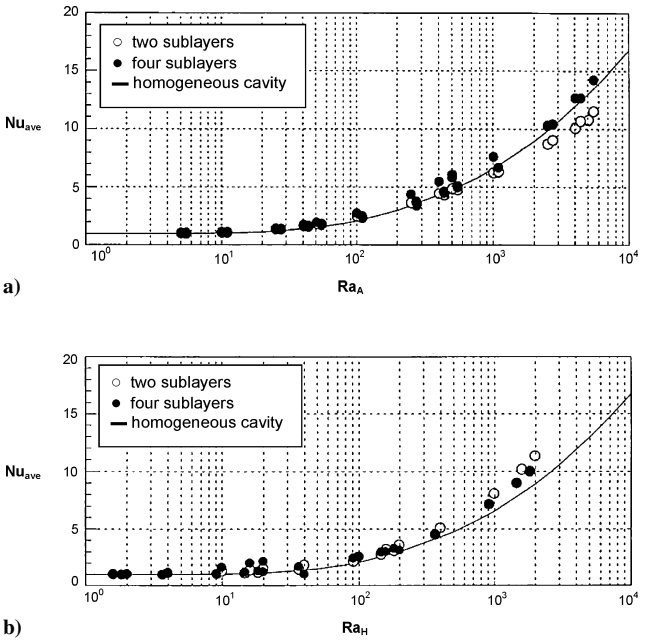

Fig. 10 Heat-transfer results for a tall porous cavity ($A = 5$): a) vertical sublayers and b) horizontal sublayers.

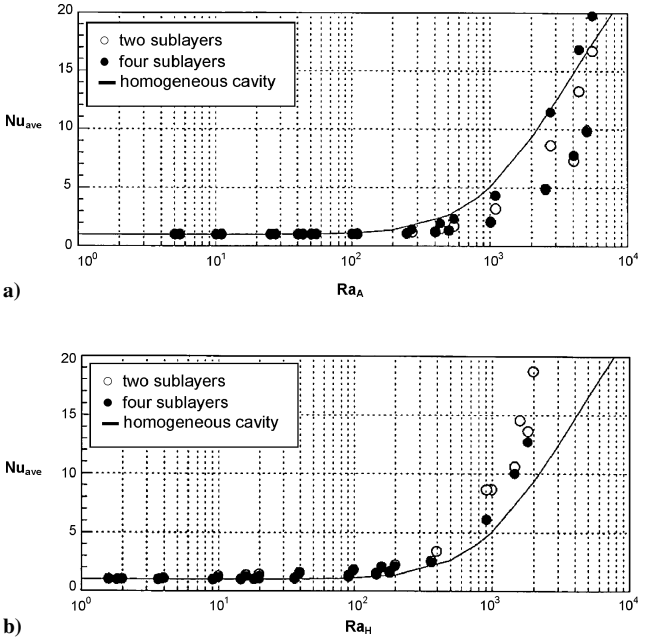

Fig. 11 Heat-transfer results for a shallow porous cavity ($A = 0.2$): a) vertical sublayers and b) horizontal sublayers.

curve given by a homogeneous cavity. This implies that the effective permeability model proposed by Leong and Lai[14] is applicable to cavities with a large range of aspect ratios. For tall cavities (Fig. 10), the maximum difference between the lumped-system prediction and that of homogeneous case is less than 15%, although it can be as high as 40% for shallow cavities (Fig. 11). Although the latter might seem a little bit high, this only occurs at a high Rayleigh number (>500). From Figs. 10 and 11, one can clearly observe that the lumped-system predicts a lower bound for shallow cavities with vertical sublayers and an upper bound for those with horizontal sublayers. For many applications where a quick estimate of heat transfer from a layered porous system is needed, the lumped-system approach will remain useful.

Conclusions

Natural convection in rectangular, layered porous cavities has been numerically examined in this study as an extension to several earlier studies.[9,10,13,14] Although most fluid flow and heat-transfer phenomena observed here are similar to those reported in a square layered cavity, the additional dimension considered in the present study provides us an opportunity to closely examine the transition of flow regime and heat-transfer mechanism when the governing parameters change. Particularly, without resorting to the boundary-layer approximation, the present results are believed to be less restricted than the results reported earlier. In addition, the present study has further examined the lumped-system approach used in the prediction of heat transfer from layered porous cavities. The results have confirmed that the lumped-system approach is generally applicable to porous cavities with any aspect ratio. Particularly, the lumped-system approach (when used with an appropriate effective permeability) works well with the tall cavities where the heat flow direction in each sublayer is mainly one dimensional and parallel to that of the primary temperature gradient. However, this approach is less successful when it is applied to a shallow cavity subject to a high Rayleigh number (>500). The reason for its poor performance is because the heat flow direction in each sublayer might no longer be one dimensional. The "leakage" of heat flow from an individual sublayer leads to a substantial deviation from the thermal circuit model on which the lumped system was based. Nevertheless the lumped-system approach will remain useful in applications. It predicts a lower bound for shallow cavities with vertical sublayers and an upper bound for those with horizontal sublayers, which should be valuable for engineers in the field.

References

[1]Masuoka, T., Katsuhara, T., Nakazono, Y., and Isozaki, S., "Onset of Convection and Flow Patterns in a Porous Layer of Two Different Media," *Heat Transfer Japanese Research*, Vol. 7, No. 1, 1978, pp. 39–52.

[2]McKibbin, R., and O'Sullivan, M. J., "Onset of Convection in a Layered Porous Medium Heated from Below," *Journal of Fluid Mechanics*, Vol. 96, Jan. 1980, pp. 375–393.

[3]Rees, D. A. S., and Riley, D. S., "The Three-Dimensional Stability of Finite-Amplitude Convection in a Layered Porous Medium Heated from Below," *Journal of Fluid Mechanics*, Vol. 211, Feb. 1990, pp. 437–461.

[4]Donaldson, I. G., "Temperature Gradients in the Upper Layers of the Earth's Crust Due to Convective Water Flows," *Journal of Geophysical Research*, Vol. 67, No. 9, 1962, pp. 3449–3459.

[5]Rana, R., Horne, R. N., and Cheng, P., "Natural Convection in a Multi-Layered Geothermal Reservoir," *Journal of Heat Transfer*, Vol. 101, No. 3, 1979, pp. 411–416.

[6]McKibbin, R., "Some Effects of Non-Homogeneity in the 'Water-Saturated Porous Layer' Model of a Geothermal Field," *Mathematics and Models in Engineering Science*, DSIR, Wellington, New Zealand, 1982, pp. 139–148.

[7]McKibbin, R., and Tyvand, P. A., "Thermal Convection in a Porous Medium Composed of Alternating Thick and Thin Layers," *International Journal of Heat and Mass Transfer*, Vol. 26, No. 5, 1983, pp. 761–780.

[8]McKibbin, R., and Tyvand, P. A., "Thermal Convection in a Porous Medium with Horizontal Cracks," *International Journal of Heat and Mass Transfer*, Vol. 27, No. 7, 1984, pp. 1007–1023.

[9]Poulikakos, D., and Bejan, A., "Natural Convection in Vertically and Horizontally Layered Porous Media Heated from the Side," *International Journal of Heat and Mass Transfer*, Vol. 26, No. 12, 1983, pp. 1805–1814.

[10]Lai, F. C., and Kulacki, F. A., "Natural Convection Across a Vertical Layered Porous Cavity," *International Journal of Heat and Mass Transfer*, Vol. 31, No. 6, 1988, pp. 1247–1260.

[11]Muralidhar, K., Baunchalk, R. A., and Kulacki, F. A., "Natural Convection in a Horizontal Porous Annulus with a Step Distribution in Permeability," *Journal of Heat Transfer*, Vol. 108, No. 4, 1986, pp. 889–893.

[12]Pan, C. P., and Lai, F. C., "Reexamination of Natural Convection in a Horizontal Layered Porous Annulus," *Journal of Heat Transfer*, Vol. 118, No. 4, 1996, pp. 990–992.

[13]Rees, D. A. S., "Free Convection Boundary Layer Flow from a Heated Surface in a Layered Porous Medium," *Journal of Porous Media*, Vol. 2, No. 1, 1999, pp. 39–58.

[14]Leong, J. C., and Lai, F. C., "Effective Permeability of a Layered Porous Cavity," *Journal of Heat Transfer*, Vol. 123, No. 3, 2001, pp. 512–519.

[15]Prasad, V., and Kulacki, F. A., "Convective Heat Transfer in a Rectangular Porous Cavity—Effect of Aspect Ratio on Flow Structure and Heat Transfer," *Journal of Heat Transfer*, Vol. 106, No. 1, 1984, pp. 158–165.